Astron. Astrophys. 335, 573–582 (1998)

ASTRONOMY AND ASTROPHYSICS

On some properties of very metal-rich stars

N. Mowlavi[1], **G. Meynet**[1], **A. Maeder**[1], **D. Schaerer**[2], **and C. Charbonnel**[3]

[1] Geneva Observatory, CH-1290 Sauverny, Switzerland
[2] Space Telescope Science Institute, 3700 San Martin Drive, Baltimore, MD 21218, USA
[3] Laboratoire d'Astrophysique de Toulouse, CNRS - UMR 5572, 14 av. E. Belin, F-31400 Toulouse, France

Received 30 September 1997 / Accepted 6 April 1998

Abstract. An analysis of some properties of stellar models as a function of metallicity Z (and helium content Y) is presented, with special attention to those stars with metallicities higher than twice or three times solar.

It is shown that the stellar properties as a function of Z are mainly determined by the effects of the opacities at sub-solar metallicities, and by the effects of the mean molecular weight and stellar mass loss at higher metallicities. As a result, very metal-rich stars ($Z \gtrsim 0.05$) exhibit properties that deviate from what is expected from the known characteristics at lower metallicities. In particular, they are more luminous and hotter than those at $Z \lesssim 0.05$ due to the effect of the mean molecular weight. They have main sequence lifetimes much shorter (60% shorter at $Z = 0.1$ than at $Z = 0.02$) than those at solar metallicity due to their lower initial hydrogen content. Finally, the high mass loss rates at high metallicities affect significantly the population synthesis of massive stars in very metal-rich regions. An analysis of expected Wolf-Rayet and supernovae populations in such conditions is briefly presented.

Key words: stars: evolution – stars: general – stars: Hertzsprung-Russell(HR) diagram – Galaxy: center – stars: Wolf-Rayet

1. Introduction

Observations as well as models of galactic chemical evolution suggest that the metallicity at the center of our galaxy, where the density of matter is high, can reach up to 3 to 5 times the solar metallicity (McWilliam & Rich 1994, Simpson et al. 1995). Other objects such as elliptical galaxies, or maybe even quasars (Korista et al. 1996), also show evidences of very metal-rich stellar populations.

The metallicity affects the evolution of stars mainly through its impact on the radiative opacities, the equation of state, the nuclear reaction rates and the stellar mass loss rates. The impact of the metallicity on the stellar properties has been well studied for $0.001 \leq Z \leq 0.04$ on base of extensive stellar model calculations (see e.g. Schaller et al. 1992, hereafter Paper I, and Maeder & Conti 1994). In contrast, they are still poorly known at metallicities much higher than solar. Recent calculations have been performed at metallicities five times solar (Fagotto et al. 1994, Mowlavi et al. 1997). Mowlavi et al. (1997) notice that those very metal-rich models present specific properties which are distinct from the ones at $Z \leq 0.04$. In particular, they are *hotter* and *more luminous* that those at solar metallicity, contrary to expectations. It is the purpose of this paper to analyze in detail some of these properties of very metal-rich stars. These could have important consequences on the observable properties of high metal-rich galaxies.

The study is based on the extensive grids of stellar models computed by the Geneva group with $0.001 \leq Z \leq 0.1$. It covers the main phases of stellar evolution, excluding the latest stages of evolution. The core helium burning phase of very metal-rich low-mass ($M < 1.7\,\mathrm{M}_\odot$) stars, important for the study of elliptical galaxies, is not considered in this paper as it has been the subject of existing papers in the literature (see, for example, Dorman, Rood & O'Connell, 1993, Fagotto et al. 1994).

A general discussion on the dependence of stellar properties on chemical composition is presented in Sect. 2. Sect. 3 summarizes the model ingredients used in the computation of the Geneva grids. The stellar properties during the main sequence (MS) and the core helium burning (CHeB) phase are analyzed in Sects. 4 and 5, respectively. Wolf-Rayet stars in very metal-rich environments are briefly discussed in Sect. 6. Conclusions are drawn in Sect. 7.

2. Chemical composition and stellar properties

Chemical composition is traditionally described by X, Y and Z, which are the mass fractions of hydrogen, helium and heavier elements, respectively. In the course of galactic evolution, the interstellar matter is progressively enriched in heavy elements, and Z increases through time. It is evident that helium is also enriched, the increase of its interstellar abundance with respect to Z being conveniently described by a $\Delta Y/\Delta Z$ law such that $Y = Y_0 + \Delta Y/\Delta Z \times Z$ (where Y_0 is the primordial He abundance). At low metallicities ($Z \lesssim 0.02$), Y remains practically constant [an absolute variation δZ of the metallicity induces an absolute variation of He of $\delta Y = \Delta Y/\Delta Z \times \delta Z$, so that $\delta Y/Y \lesssim 10^{-2}$ for $Z \lesssim 10^{-3}$], and the stellar properties *as a function of metallicity* are thus expected to be determined mainly by Z. At high metallicities ($Z \gtrsim 0.02$), on the other

hand, Y increases (or, alternatively, X decreases) significantly with Z (Y passes from 0.30 to 0.48 when Z increases from 0.02 to 0.1, see Table 1). In those conditions, both Z *and* Y (and $X = 1 - Y - Z$) determine the stellar properties as a function of metallicity.

Chemical composition influences the stellar structure basically through three contributions: the mean molecular weight μ, the radiative opacity κ, and the nuclear energy production ε_{nuc}. The metallicity-dependent mass loss rate $\dot{M}$ further affects stellar evolution as a function of Z.

2.1. The μ-effect

The mean molecular weight acts in the hydrostatic equilibrium of the star. Let us imagine a *thought experiment* in which μ is arbitrarily increased over the whole star, all other quantities such as κ or ε being unaltered (though keeping, of course, their density and temperature dependences). The reduction in the gas pressure leads to an overall contraction (and heating) until hydrostatic equilibrium is re-established. As a result, the stellar radius decreases and the surface temperature T_{eff} increases. The surface luminosity L, on the other hand, increases with μ since $L(r) \propto T^3 \, \mathrm{d}T/\mathrm{d}r$ [in the case of radiative transfer, with $L(r)$ and T being the luminosity and temperature at radius r, respectively]. In summary, *an increase in* μ *tends to increase both* L *and* T_{eff}.

This μ-effect is undetectable in low-metallicity stars, where μ is essentially constant as a function of metallicity. At metallicities higher than about solar, however, μ increases as a result of increasing Y [Z remains unimportant in this respect for all realistic values of Z, since $\mu \simeq (2X + 0.75Y + 0.5Z)^{-1}$]. And indeed, it is shown in Sects. 4 and 5 that very metal-rich models are more luminous and hotter than solar-metallicity ones. It has to be noted that the $\Delta Y/\Delta Z$ law adopted in metal-rich models has an important influence in this respect, as it fixes Y and thus μ.

2.2. The κ-effect

The radiative opacity acts in the (radiative) transport of energy. Let us consider again a *thought experiment* in which the opacity is arbitrarily increased throughout the star, all other quantities (such as μ or ε_{nuc}) being unaltered. The hydrostatic structure remains unaffected to first approximation. In particular the radius and temperature profiles are unchanged. The energy flux, on the other hand, decreases with increasing κ [since $L(r) \propto \kappa^{-1} \, T^3 \, \mathrm{d}T/\mathrm{d}r$ for radiative transfer], leading to a decrease in the surface luminosity. As the radius is unaffected to first order, the surface temperature decreases too. In summary, *an increase in* κ *tends to decrease both* L *and* T_{eff}.

In general, the opacities increase with increasing metallicity. This is the case for the bound-free (see Eq. 16.107 in Cox & Giuli 1969) and free-free (see Eq. 16.95 in Cox & Giuli 1969) transitions. In contrast, electron scattering depends only on X [$\kappa_e \simeq 0.20(1 + X)$], which is about constant at $Z \lesssim 0.01$ and decreases with Z at $Z \gtrsim 0.01$. As seen in Sect. 4, these considerations explain the stellar properties as a function of Z at sub-solar metallicities.

2.3. The ε_{nuc}-effect

The nuclear energy production ε_{nuc} sustains the stellar luminosity. If ε_{nuc} is arbitrarily increased, the central regions of the star expand, leading to a decrease in the temperatures and densities, and to an increase in the stellar radius. Thus, *an increase in* ε_{nuc} *tends to decrease both* L *and* T_{eff}, as well as the central temperature T_c and density ρ_c.

The way ε_{nuc} depends on metallicity is closely related to the mode of nuclear burning. When the CNO cycles are the main mode of H burning, ε_{nuc} increases with Z. In contrast, when the main mode of burning is the pp chain, ε_{nuc} is related to X. It is thus about independent of Z at $Z \lesssim 0.02$, and decreases with increasing Z at $Z \gtrsim 0.02$. As shown in Sect. 4, these properties determine the behavior of T_c and ρ_c in MS stars as a function of Z.

2.4. The effect of $\dot{M}$

When mass loss is driven by radiation, Kudritzki et al. (1989) showed that $\dot{M}$ in O stars is proportional to $Z^{0.5}$. As a result, the effects of mass loss dominate in more metal-rich stars. Mass loss reduces the stellar mass, modifying thereby the post-MS stellar properties (and even during the MS for the most massive ones). It also turns the (massive) star into a Wolf-Rayet star at an earlier stage than it would at lower metallicity. This is analysed in more detail in Sect. 6.

2.5. Summary

At $Z \lesssim 0.02$, Z is the main factor acting through the κ-effect. The adopted $\Delta Y/\Delta Z$ law is thus not influential. At $Z \gtrsim 0.02$, on the other hand, Y plays a dominant role mainly through the μ-effect, while Z acts on the mass loss rate. The adopted $\Delta Y/\Delta Z$ law is then important.

These combined effects of μ, κ and ε_{nuc} on the stellar surface properties can be estimated more quantitatively with a semi-analytical approach using homology relations. This is developed in the appendix for a $3\,\mathrm{M}_\odot$ star. A more detailed analysis of stellar properties with metallicity, however, can only be done with the help of stellar model calculations. Such analysis is provided in Sects. 4 and 5 using the Geneva grids of models, whose ingredients are first summarized in the next section.

3. Models

The stellar grids published by the Geneva group from $Z = 0.001$ to 0.1 (summarized in Table 1) constitute a homogeneous set of models. They are computed with a value of $\alpha_p = l/H_p = 1.6$ for the ratio of the mixing length l in convective regions to the pressure scale height H_p (determined in order to match the sun and the location of the red giant branch in the HR diagram), and a moderate core overshooting distance of $d = 0.20 \; H_p$

Table 1. Geneva group grids of models (see text)

Grid$^{(*)}$	Z	X	Y	$\dot{M}$	Interior opacities	Low T opacities
I	0.001	0.756	0.243	standard	Rogers & Iglesias (1992)	Kurucz (1991)
III	0.004	0.744	0.252	standard	Iglesias et al. (1992)	Kurucz (1991)
II	0.008	0.728	0.264	standard	Rogers & Iglesias (1992)	Kurucz (1991)
I	0.020	0.680	0.300	standard	Rogers & Iglesias (1992)	Kurucz (1991)
IV	0.040	0.620	0.340	standard	Iglesias et al. (1992)	Kurucz (1991)
VII	0.100	0.420	0.480	standard	Iglesias & Rogers (1996)	Alexander & Fergusson (1994)
V	$0.001 \rightarrow 0.04$	$M \geq 12\,M_\odot$		$2\times$standard	Iglesias et al. (1992)	Kurucz (1991)

$^{(*)}$ I : Schaller et al. (1992, Paper I); IV : Schaerer et al. (1993, Paper IV);
II : Schaerer et al. (1993, Paper II); V : Meynet et al. (1994, Paper V);
III: Charbonnel et al. (1993, Paper III); VII: Mowlavi et al. (1997, Paper VII).

beyond the classical convective core boundary as defined by the Schwarzschild criterion (in order to reproduce the MS width in the HR diagram). We refer to Paper I (see Table 1 for the references of the papers) for a general description of the physical ingredients. We mention below only the specific ingredients which differ from one set of calculations to another.

The primordial helium abundance Y_0 is taken equal to 0.24 (cf. Audouze 1987) for all models. The relative ratio of helium to metal enrichment, on the other hand, is $\Delta Y/\Delta Z = 3$ at $Z \leq 0.02$, 2.5 at $Z = 0.04$, and 2.4 at $Z = 0.1$. At low metallicity, the model output is not very sensitive to the adopted value for $\Delta Y/\Delta Z$. At $Z \gtrsim 0.02$, however, the model output is sensitive to $\Delta Y/\Delta Z$ (see Sect. 2). The values adopted at $Z = 0.04$ and 0.1 are consistent with the currently admitted value of ~ 2.5 (see Peimbert 1995 and references therein), but the uncertainties are still very high (Maeder 1998).

The grids presented in Papers I to VII are all calculated with the OPAL opacities. They use, however, different OPAL tables according to their availability at the time of each calculation, which are summarized in Table 1. The low temperature opacities are taken from Kurucz (1991) in all grids, except in Paper VII which uses the Alexander & Ferguson (1994) tables.

The mass loss prescription is of crucial importance for the evolution of the models. A general dependence of $\dot{M} \propto Z^{0.5}$, as suggested by the models of Kudritzki et al. (1989), is adopted for all the stars except the WR stars. A Reimers law (1975) is adopted in all grids for low- and intermediate-mass stars. For massive stars, the situation is more delicate. In a first set of calculations (Papers I to IV), mass loss rates from de Jager et al. (1988, 'standard' mass loss rates) were used. A second set of calculations (Paper V) were then performed with enhanced mass loss rates during the pre-WR and WNL phases (by a factor of two over the 'standard' ones). The latter models were found to better reproduce many observational constraints concerning massive stars (Maeder & Meynet 1994), and we use them in this paper too. At $Z = 0.1$, however, the standard mass loss rates for massive stars are used (Paper VII). Indeed, we expect the mass loss rates driven by radiation pressure to be probably saturated at such high metallicities. The conclusions are, however, qualitatively not affected by this choice.

Let us recall that at $Z = 0.1$, the criterion defining a star to be of the Wolf-Rayet type could be different from that at lower metallicities. However, in the absence of any observational counterpart of those objects at such high metallicities, we keep the same criterion as in Paper I, i.e. we consider that a star enters the WR stage when its surface hydrogen mass fraction becomes lower than 0.4 and its effective temperature is higher than 10000 K. These values are actually not crucial for the analysis of WR populations since the characteristic time-scale for entering the WR stage is very short compared to the WR lifetimes. The mass loss rates of these objects are then accordingly taken as in Paper I.

4. The main sequence

4.1. The zero-age main sequence

The arguments presented in Sect. 2 enable to understand the location of the zero-age main sequence (ZAMS) in the Hertzsprung-Russell (HR) diagram as a function of metallicity. That location is given in Fig. 1 for stars of 1, 3 and $20\,M_\odot$ at metallicities ranging from $Z = 0.001$ to 0.1.

Metallicities below $\simeq 0.04$*:* At $Z \lesssim 0,.4$, the surface properties (as a function of Z) are determined by the κ-effect (see Sect. 2.2). The surface temperature is mainly sensitive to the opacity in the outer layers where bound-bound and bound-free transitions dominate, so that all ZAMS models get cooler with increasing metallicities. The surface luminosity, on the other hand, is sensitive to the interior opacities. In low- and intermediate-mass stars, the main source of opacity is provided by bound-free transitions, and increases with metallicity. As a result, L decreases with Z. In massive stars, however, electron-scattering is the main source of opacity. As this source is metallicity independent, the luminosity of low-metallicity massive stars is insensitive to Z.

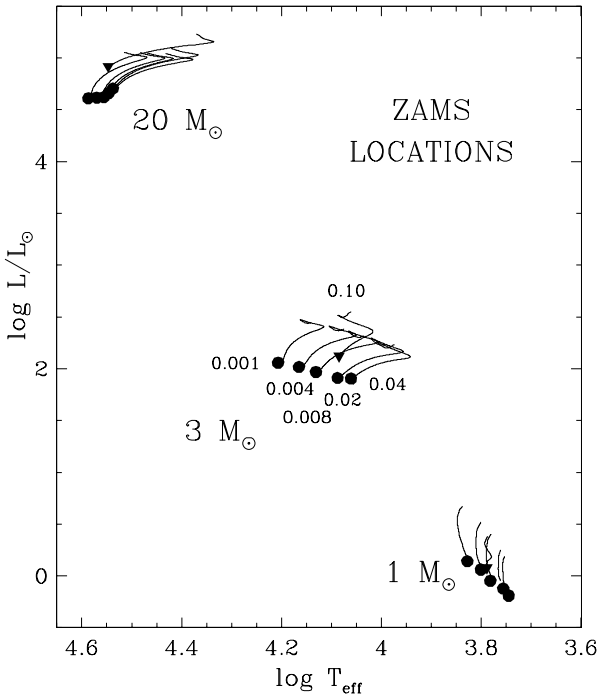

Fig. 1. ZAMS locations in the HR diagram of 1, 3 and $20\,\mathrm{M}_\odot$ star models at different metallicities as labeled in the figure for the $3\,\mathrm{M}_\odot$ star. Models at $Z = 0.1$ are identified by triangles. The models are computed with OPAL and Alexander & Ferguson (1994) opacities

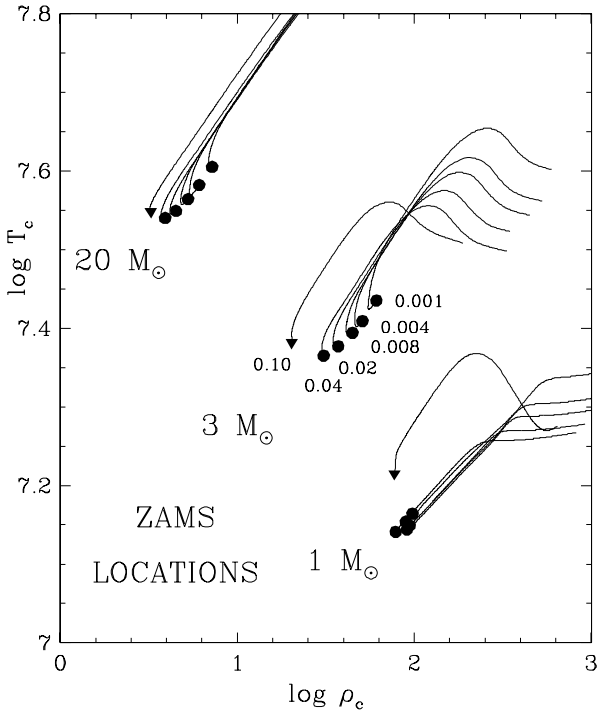

Fig. 2. Same as Fig. 1 but in the $(\log \rho_c, \log T_c)$ diagram

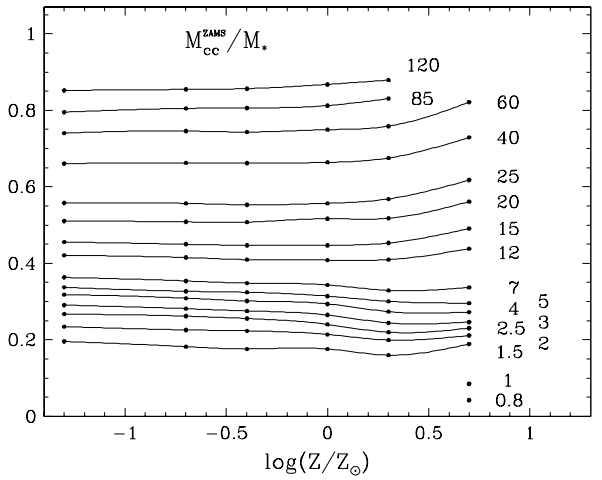

Fig. 3. Masses of convective cores relative to the stellar masses as labeled (in solar masses) next to the curves, as a function of metallicity

Metal-rich stars: As the metallicity increases above $Z \simeq 0.02$, the μ-effect becomes competitive with the κ-effect. In low- and intermediate-mass stars, the μ-effect eventually exceeds the κ-effect above $Z \simeq 0.05$, and a further increase in the metallicity results in *hotter* and *more luminous*[1]. ZAMS models (see Sect. 2.1). In massive stars, L already begins to increase as a function of Z at $Z \simeq 0.02$ since the κ-effect on L is negligible in those stars.

Let us now consider the central temperature T_c and density ρ_c. Those quantities are, contrarily to L and T_{eff}, closely related to the nuclear energetic properties of the core material (see Sect. 2.3). In particular, they are sensitive to the mode of hydrogen burning. Usually, the CNO cycles are the main mode of core H burning for stars more massive than about $1.15 - 1.30\,\mathrm{M}_\odot$ (depending on metallicity), while the pp chain operates at lower masses. At $Z = 0.1$, however, all stars are found to burn their hydrogen through the CNO cycles (at least down to $M = 0.8\,\mathrm{M}_\odot$ considered in our grids).

When the CNO cycle is the main mode of burning, ρ_c and T_c decrease with increasing Z (see Sect. 2.3). This is clearly visible in Fig. 2 for the 3 and $20\,\mathrm{M}_\odot$ stars at $Z \leq 0.04$. At $Z = 0.1$, however, the higher surface luminosities of the models as compared to those at $Z = 0.04$ result in concomitant higher central temperatures.

[1] These properties remained unnoticed by Fagotto et al. (1994), though inspection of the data available from their tables reveal that their results indeed support our conclusions.

When the pp chain is the main mode of burning, on the other hand, the location in the $(\log \rho_c, \log T_c)$ is not very sensitive to Z. This is well verified for the $1\,\mathrm{M}_\odot$ models at $Z < 0.1$ (Fig. 2).

4.2. Main sequence convective core sizes

The mass of the convective core is mainly determined by the nuclear energy production, and thus by L. At $Z \lesssim 0.04$, it slightly decreases with increasing Z in low- and intermediate-mass stars, while it remains approximately constant in massive stars (see Fig. 3). At $Z \gtrsim 0.04$, on the other hand, it increases

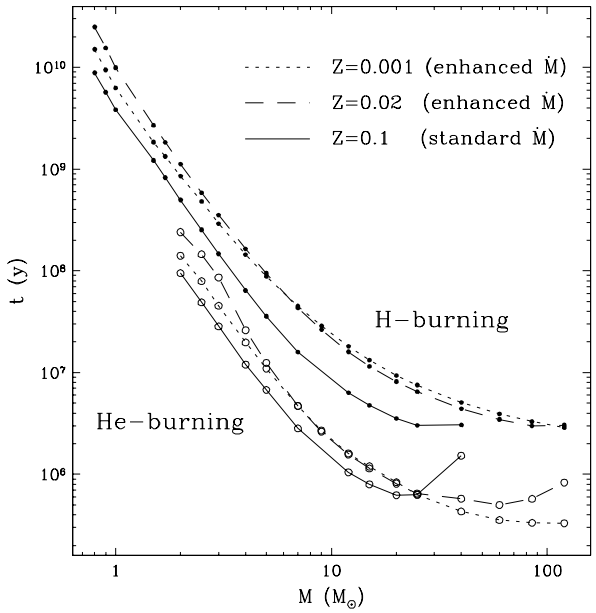

Fig. 4. Main sequence (filled circles) and core helium burning (open circles) lifetimes of Z=0.001 (dotted lines), 0.02 (dashed lines) and 0.1 (solid lines) models as a function of their initial mass

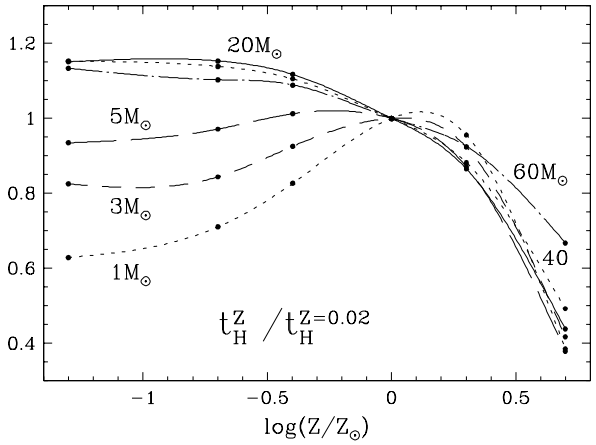

Fig. 5. Main sequence lifetimes of models of initial masses as labeled on the curves, as a function of their metallicity. The lifetimes are normalized for each stellar mass to its value at $Z = 0.02$

with Z at all stellar masses[2]. We recall furthermore that at $Z = 0.1$ all stars with M as low as $0.8\,\mathrm{M}_\odot$ possess convective cores.

4.3. Main sequence lifetimes

The MS lifetimes t_H are summarized in Fig. 4 for three different metallicities as a function of the initial stellar mass, and in Fig. 5 for several stellar masses as a function of metallicity.

[2] It is interesting to note that we could have expected smaller convective cores in metal-rich massive stars where the main source of opacity is electron scattering (since this opacity is positively correlated with the H content). But the effect of higher luminosity in those stars overcomes that κ-effect, and the core mass increases with increasing Z.

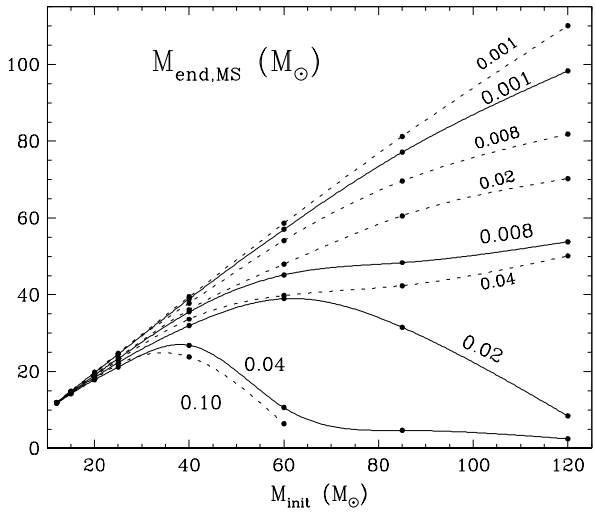

Fig. 6. Stellar masses at the end of the main sequence phase as a function of initial mass for different metallicities as labeled on the curves. Dotted lines correspond to models computed with the 'standard' mass loss rates for massive stars (Papers I to IV and VII), while thick lines correspond to models computed with twice that 'standard' mass loss rates (Paper V)

They can be understood in terms of two factors: the initial H abundance, which determines the quantity of available fuel, and the luminosity of the star, which fixes the rate at which this fuel burns.

At $Z \lesssim 0.02$, t_H is mainly determined by L, being shorter at higher luminosities. Fig. 5 confirms, as expected from L (see Fig. 1), that t_H increases with Z in low- and intermediate-mass stars, and is about independent of Z in massive stars.

At $Z > 0.02$, on the other hand, the initial H abundance decreases sharply with increasing Z (the H depletion law is dictated by the adopted $\Delta Y/\Delta Z$ law; for $\Delta Y/\Delta Z = 2.4$ and $Y_0 = 0.24$, X drops from 0.69 at $Z = 0.02$ to 0.42 at $Z = 0.1$). The MS lifetimes are then mainly dictated by the amount of fuel available. This, combined with the higher luminosities at $Z = 0.1$, leads to MS lifetimes which are about 60% shorter at $Z = 0.1$ than at $Z = 0.02$. This result is independent of the stellar mass for $M \leq 40\,\mathrm{M}_\odot$. Above this mass, however, the action of mass loss extends the MS lifetime, as can be seen from the $60\,\mathrm{M}_\odot$ curve in Fig. 5.

4.4. Masses at the end of the MS phase

Mass loss determines crucially the evolution of massive stars, especially at high metallicities. The stellar masses remaining at the end of the MS phase with the 'enhanced' mass-loss prescription (see Sect. 3) are shown in thick lines in Fig. 6 (the ones with 'standard' mass-loss prescription is also shown in dotted lines for comparison). The most striking result at metallicities higher than twice solar is the rapid evaporation of massive stars with $M \gtrsim 50\,\mathrm{M}_\odot$, and the consequent formation of WR stars during core H burning. At $Z = 0.04$, stars more massive than $\sim 80\,\mathrm{M}_\odot$ leave the core hydrogen burning phase with less than

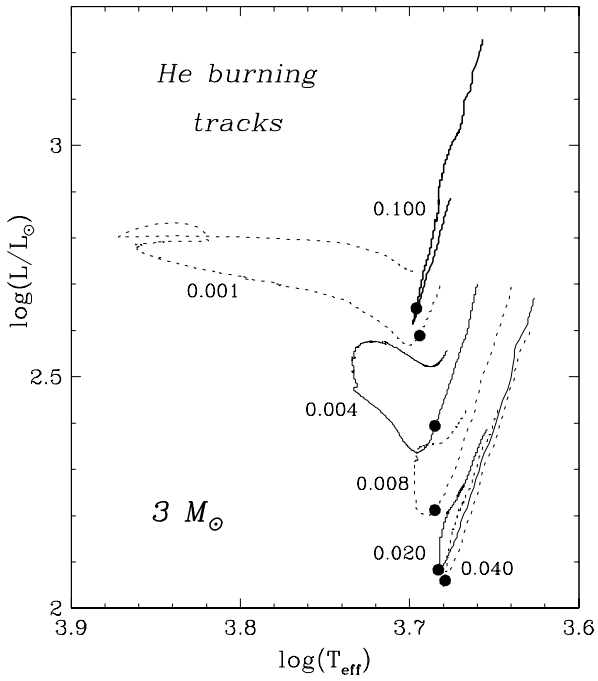

Fig. 7. Tracks followed in the HR diagram during the core helium burning phase by $3\,\mathrm{M}_\odot$ models at different metallicities as labeled in the figure. The points on each track locate the model when the core helium abundance has dropped to $X_c(^4\mathrm{He}) = 0.85$

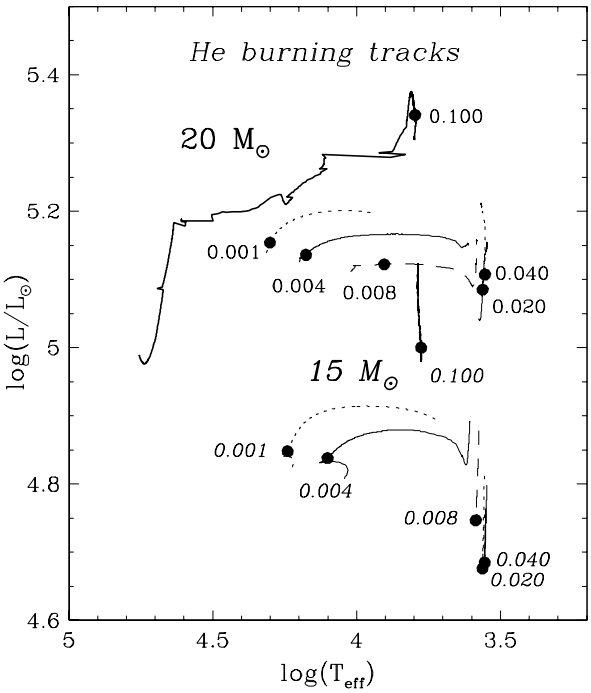

Fig. 8. Same as Fig. 7 but for the $15\,\mathrm{M}_\odot$ (labeled in italics) and $20\,\mathrm{M}_\odot$ (labeled in straight) models. Only the part following He ignition is shown

$5\,\mathrm{M}_\odot$. The same holds true at $Z = 0.1$ even though 'standard' mass loss rates are used for that metallicity.

5. The core He-burning phase

5.1. The HR diagram

The surface properties during the CHeB phase are dictated by the same arguments developed in Sect. 2 and used to explain the MS properties (see Sect. 4). At $Z \lesssim 0.04$, both L and T_{eff} decrease with increasing Z, due to the κ-effect. At $Z \gtrsim 0.04$, on the other hand, both L and T_{eff} increase with Z, due to the μ-effect. These properties are well verified in Figs. 7 and 8 which show the CHeB tracks in the HR diagram of intermediate-mass and massive stars, respectively.

Low- and intermediate-mass stars of low metallicity are known to perform a blue loop in the HR diagram and cross the Cepheid instability strip. The extent of that loop is a function of both the stellar mass (more massive stars having more extended loops) and the metallicity (more metal-rich stars having less extended blue loops). For a $3\,\mathrm{M}_\odot$ star, the blue loop is suppressed at $Z \gtrsim 0.008$ (see Fig. 7), while it is suppressed at $Z > 0.02$ for a $5\,\mathrm{M}_\odot$ star. Furthermore, no blue loop is obtained for any stellar mass at metallicities higher than $Z \simeq 0.04$.

Another interesting property is the effective temperature at which massive stars enter the CHeB phase. Low-metallicity massive star models ignite helium as blue supergiants, while solar metallicity models ignite helium as red supergiants. This location of helium ignition as a function of Z in the HR diagram is shown in Fig. 8. As a result, the number ratio of blue-to-red supergiants is a decreasing function of the metallicity[3]. We finally notice, again, the departure of $Z = 0.1$ models to the general rule: they ignite helium at a surface temperature higher than those of solar metallicity models. This is due to the μ-effect (see Sect. 2.1).

5.2. Core helium burning lifetime

The CHeB lifetime t_{He} is displayed in Fig. 4 for three different metallicities as a function of the initial stellar mass, and in Fig. 9 as a function of metallicity for several initial masses. It follows a pattern very similar to that of t_H (Fig. 5) for intermediate-mass stars, and can be understood on grounds of the same arguments developed in Sect. 4.3.

In massive stars, the CHeB lifetime is extended as a result of the lower average luminosities due to mass loss. As a result, the CHeB lifetime relative to its value at $Z = 0.02$ increases with the initial stellar mass.

The ratio t_H/t_{He} is displayed in Fig. 10. Below $Z \simeq 0.04$, this ratio is a decreasing function of metallicity, for a given stellar mass, and an increasing function of stellar mass, for a given metallicity. Above $Z \simeq 0.04$, this ratio converges to the value of $t_H/t_{He} \simeq 5.5$, irrespective of the stellar mass. For stars more massive than $\sim 30\,\mathrm{M}_\odot$, however, the high mass loss rates reduce further this ratio.

[3] Let us recall that this property is found by all existing stellar models, but is *not* supported by the observations. We refer to Langer & Maeder (1995) for a discussion on this issue.

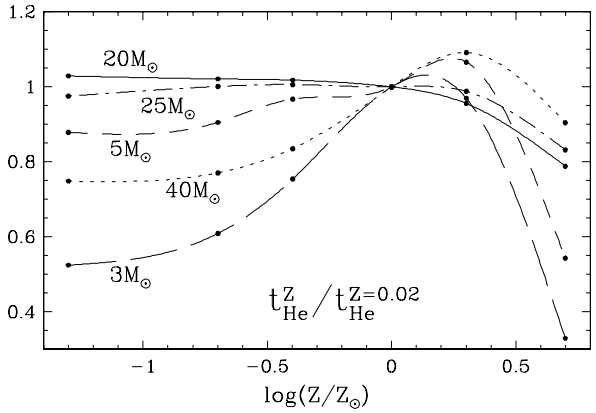

Fig. 9. Core He burning lifetimes of models of initial masses as labeled on the curves, as a function of metallicity. The lifetimes are normalized for each stellar mass to its value at $Z = 0.02$

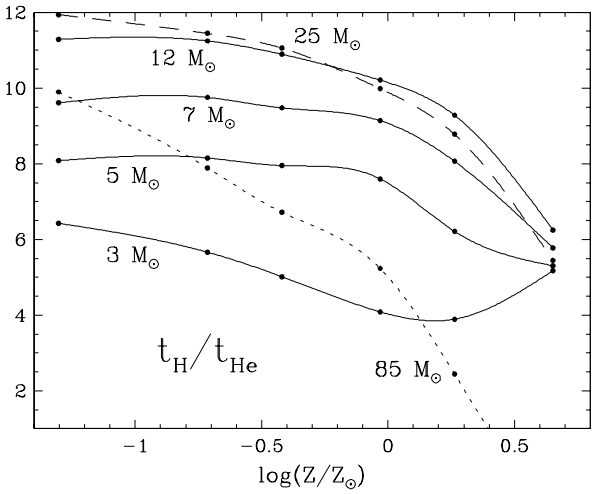

Fig. 10. Ratio of core H to core He burning lifetimes for models of initial masses as labeled on the curves, as a function of metallicity

5.3. Masses at the end of the CHeB phase

The masses at the end of the CHeB phase of massive stars are displayed in Fig. 11 for several metallicities. These are a decreasing function of increasing metallicity.

6. Wolf-Rayet stars in very metal-rich environments

The properties of the WR star models at metallicities between 0.001 and 0.04 have already been presented in Maeder & Meynet (1994). Here we shall focus our discussion on the expected characteristics of the WR stars in very metal-rich environments, i.e. at $Z = 0.1$.

The minimum initial mass for a single star to become a WR star is a decreasing function of metallicity. It goes from $25\,\mathrm{M}_\odot$ at $Z = 0.02$ to $21\,\mathrm{M}_\odot$ at $Z = 0.04$ (see Table 1 in Maeder & Meynet 1994, $2 \times \dot{M}$ case), and to approximately $17\,\mathrm{M}_\odot$ at $Z = 0.1$.

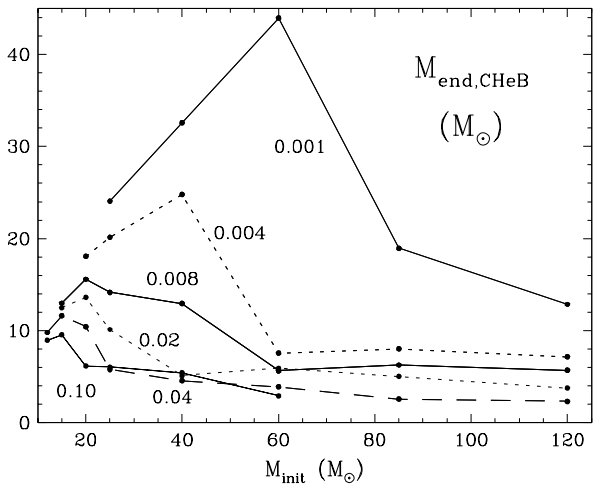

Fig. 11. Stellar masses at the end of the core helium burning phase as a function of initial mass for different metallicities as labeled on the curves. Only models computed with twice the 'standard' mass loss rates for massive stars are shown, except at $Z = 0.1$ for which the mass loss rates are 'standard'

6.1. $M_{init} \gtrsim 60\,\mathrm{M}_\odot$: ending as helium white dwarf?

At $Z = 0.1$, stars more massive than about 60 $M_\odot$ literally evaporate during the main sequence phase. They loose so much mass that they never reach the He-burning phase, and will likely end their nuclear life as helium white dwarfs. Let us remark here that helium white dwarf stars are generally thought to be the end point evolution of very low mass stars typically with initial masses between 0.08 and 0.5 $M_\odot$. Their existence in our present universe is thus doubtful (unless created through binary mass transfer), since the MS lifetimes of these very low mass stars are greater than the present age of the universe. In contrast, the above scenario (already addressed by Maeder & Lequeux 1982; see also Paper V), in which massive evaporating stars could end their stellar life as helium white dwarfs, allows the formation of such objects in young star forming regions at very high metallicities.

6.2. WN & WC Wolf-Rayet stars

Stars more massive than about 50 $M_\odot$ never enter the WC phase at $Z = 0.1$. Due to very high mass loss rates acting already during the MS, the H-convective core rapidly decreases in mass, leaving behind a great portion of the star with CNO-enriched material. As a consequence, the star goes through a very long WN phase. Moreover, these stars enter the core He-burning phase, if they do enter this phase at all, with very low masses. This implies in particular so small mass loss rates, according to the $\dot{\mathrm{M}}(\mathrm{M})$ relation proposed by Langer (1989), that their helium burning core never uncovers, preventing the star to become a WC Wolf-Rayet star.

6.3. Wolf-Rayet versus O type stars

The number ratio of WR to O type stars expected in a constant star formation rate region at $Z = 0.1$ is estimated from these models to be around 0.45. To compute this value, only the single star evolutionary channel was considered, we chose a Salpeter initial mass function (i.e. with a slope equal to 1.35), and the upper mass limit was taken equal to 60 $M_{\odot}$.

From the above result, one expects to find at $Z = 0.1$ about 1 WR star per each 2 O-type stars detected! This is a very large proportion compared to regions with solar and sub-solar metallicity (in the solar neighborhood, the observed number ratio WR/O is 0.1). This high proportion results mainly from the very high mass losses experienced by these metal-rich stars, which, as seen above, decrease the minimum initial mass for WR star formation, make the star enter the WR phase at an earlier stage of its evolution, and increase the core helium burning lifetime. Moreover, the duration of the O-type phase of metal-rich stars is considerably reduced as compared to that at lower metallicities. For instance when Z increases from 0.04 to 0.1, the lifetime of the O-type phase decreases by about a factor 2. This is essentially a consequence of the shorter duration of the H-burning phase at $Z = 0.1$ (see Fig. 5).

6.4. Supernovae

Let us now consider the final evolution of massive stars and estimate the relative fraction of supernovae with WR progenitors using some simplifying assumptions (see also Meynet et al., 1998). There is at present some uncertainties concerning the fate of WR stars, and to which type of supernovae they can give birth. As a first approximation, we make the hypothesis that all WR stars do lead to supernovae events (see a discussion in Maeder & Lequeux 1982). Moreover, since the H-rich envelope is ejected through the wind during the WNL phase, we further assume that WNE and WC stars result in supernovae of type I (whether Ib, Ic, or another yet unknown subclassification). With these assumptions, and not considering type Ia supernovae which have low-mass progenitors, one expects that metal-rich regions be characterized by a higher fraction of type I(b/c) supernovae relative to the total number of supernovae (Maeder 1992). As a numerical example, using the same IMF as in Sect. 6.3 and making the hypothesis of constant star formation rate, one obtains that, at $Z = 0.1$, the fraction of supernovae with WNE-WC progenitors amounts to 32% of the total number of supernovae having massive star progenitors. In other words, 1 supernova event out of 3 should be of type I(b/c) in very metal-rich regions. For comparison, this proportion decreases to 1 WR explosion per $5 - 7$ supernovae at solar metallicity.

7. Conclusions

This paper analyzes some properties of stellar models as a function of the metallicity, with particular attention to those at very high metallicities (above twice or three times solar). The stellar properties as a function of Z are shown to result from the action of four ingredients[4]: the mean molecular weight, an increase of which leads to more luminous and hotter stars (the μ-effect); the opacity, an increase of which leads to less luminous and cooler stars (the κ-effect); the nuclear energy production (but to a lesser extent), an increase of which leads to less luminous and cooler stars with lower T_c and ρ_c (the ε_{nuc}-effect; and mass loss, which acts indirectly on the stellar structure by reducing the stellar mass (dramatically in the most massive metal-rich stars). The κ-effect plays the main role at $Z \lesssim 0.04$, while the μ-effect becomes preponderant at $Z \gtrsim 0.02$. In the later case, the $\Delta Y/\Delta Z$ law is important.

Based on these considerations and on the Geneva's grids of stellar models, it is shown in particular that very metal-rich stars exhibit properties which cannot be extrapolated from model characteristics at lower metallicities. In particular,
- very metal-rich stars (such as at $Z = 0.1$) are more luminous and hotter than those at $Z \leq 0.05$. This property contrasts with the usually known trend at lower metallicities (whereby L and T_{eff} decrease with increasing Z due to the κ-effect);
- very metal-rich stars have much lower MS lifetimes than those at $Z \leq 0.05$. For example the MS lifetime at $Z = 0.1$ is 2.5 times shorter than that at solar metallicity, independent of their initial mass (at least up to $40\,\mathrm{M}_{\odot}$);
- stellar population synthesis in metal-rich environments is significantly affected by the increased mass loss rates at high Z. In particular, a) massive stars with $Z = 0.1$ enter the WNL Wolf-Rayet phase very early during their evolution, and those more massive than about $50\,\mathrm{M}_{\odot}$ probably never enter the WC phase; b) the most massive ($M \geq 60\,\mathrm{M}_{\odot}$ at $Z = 0.1$) high-metallicity stars loose the majority of their mass during their MS phase, and probably end their life as He white dwarfs; and c) the number of WR stars over O-type stars increases with metallicity, and metal-rich regions are expected to be characterized by a high fraction of type I (b/c/other?) supernovae relative to the total number of supernovae having massive star progenitors (up to 1 out of 3 core collapse supernovae events at $Z = 0.1$).

Appendix A: the ZAMS location in the HR diagram as a function of metallicity: a semi-analytical approach

The luminosity and effective temperature on the zero age main sequence (ZAMS) are given by the homology relations (see, for example, Cox and Giuli 1969, p 696)

$$L \propto \epsilon_0^{-0.02}{}^{-0.08} \kappa_0^{-1.02}{}^{-1.08} \mu^{7.3}{}_{7.8} M^{5.2}{}_{5.5} \tag{A1}$$

and

$$T_{eff} \propto \epsilon_0^{-0.03}{}^{-0.10} \kappa_0^{-0.28}{}^{-0.35} \mu^{1.6}{}_{2.2} M^{0.94}{}_{1.33} \tag{A2}$$

where μ and M are the mean molecular weight and the stellar mass, respectively, ϵ_0 the temperature and density independent coefficient in the relation for the nuclear energy production

[4] We neglect in this paper the effects of mild mixing processes due for example to rotation, diffusion, gravitational settling, etc... which may modify the internal composition profiles and some of the values given here

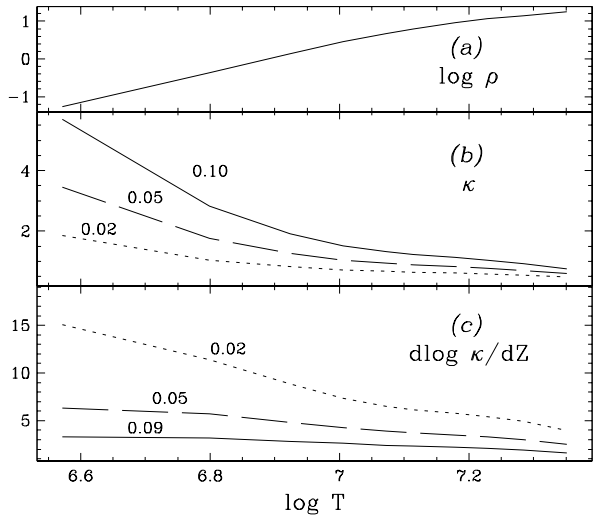

Fig. A1. a Density profile as a function of temperature in a ZAMS model of a $3\,\mathrm{M}_\odot$ stars at $Z = 0.1$; **b** Opacity profiles, as a function of temperature, at three metallicities as labeled on the curves, and calculated from the tables of Iglesias & Rogers (1996) at the densities displayed in (a); **c** Same as **b**, but for the derivative $\mathrm{d}\log\kappa/\mathrm{d}Z$ at the labeled metallicities. The derivative is calculated numerically from $(\log\kappa^{Z+0.01} - \log\kappa^{Z-0.01})/0.02$

$\epsilon_{nuc} = \epsilon_0\ \rho^\lambda\ T^\nu$ (see Cox and Giuli 1969, p 692), and κ_0 the opacity coefficient in the Kramers law $\kappa = \kappa_0\ \rho\ T^{-3.5}$. The numbers on the first line of the superscripts in Eqs. A1 and A2 apply when the nuclear energy production results from the pp chain, while the second line applies when the CNO cycles provide the main source of nuclear energy.

A variation ΔZ in the metallicity of a star of mass M affects its position in the HR diagram by

$$\Delta\log L = \left\{\begin{array}{c}7.3\\7.8\end{array}\right\}\Delta\log\mu - \left\{\begin{array}{c}1.02\\1.08\end{array}\right\}\Delta\log\kappa_0 - \left\{\begin{array}{c}0.02\\0.08\end{array}\right\}\Delta\log\epsilon_0 \quad \text{(A3)}$$

$$\Delta\log T_{eff} = \left\{\begin{array}{c}1.6\\2.2\end{array}\right\}\Delta\log\mu - \left\{\begin{array}{c}0.28\\0.35\end{array}\right\}\Delta\log\kappa_0 - \left\{\begin{array}{c}0.03\\0.10\end{array}\right\}\Delta\log\epsilon_0 \quad \text{(A4)}$$

The variation of μ is easily related to that of Z:

$$\Delta\log\mu = \frac{4.5}{\ln 10}\mu\Delta Z \quad \text{(A5)}$$

where we have used the relations

$$Y = 0.24 + 2.4Z \quad \text{(A6)}$$

and

$$X + Y + Z = 1. \quad \text{(A7)}$$

The variation of $\Delta\log\kappa_0$ as a factor of ΔZ is more difficult to evaluate. We can get an estimation of $\Delta\log\kappa_0/\Delta Z$ by comparing the opacities given by the Rogers and Iglesias (1992) tables at different metallicities. The opacities at $Z = 0.02$, 0.06 and 0.1 (and at X, Y given by Eqs. A6 and A7) are shown in Fig. A1(b) for temperature and density conditions representative of the interior of a $3\,\mathrm{M}_\odot$, $Z = 0.1$ ZAMS model [Fig. A1(a); we assume, as a first approximation, that the same $\rho - T$ profile applies at those three metallicities]. If the opacity profile were following a Kramers law, then the derivative $\mathrm{d}\log\kappa/\mathrm{d}Z$ would be constant and equal to that of the Kramers opacity coefficient $\mathrm{d}\log\kappa_0/\mathrm{d}Z$ (ρ and T being held constant). Inspection of Fig. A1(c) shows that this is obviously not the case. The derivative is seen to vary from 4 to 15 at $Z = 0.02$ and from 1.5 to 3.3 at $Z = 0.09$. However in this order of magnitude approach, we consider mean values equal

$$\Delta\log\kappa_0 \simeq 10\Delta Z \qquad \mathrm{Z} = 0.02 \quad \text{(A8)}$$

$$\Delta\log\kappa_0 \simeq 2.5\Delta Z \qquad \mathrm{Z} = 0.1 \quad \text{(A9)}$$

The variation of $\Delta\log\epsilon_0$ as a function of heavy element abundances ΔZ can be estimated knowing that the CN cycle is the main energy producer in the $3\,\mathrm{M}_\odot$ star (see e.g. Mowlavi 1995, Fig. A.3). The two reactions $^{12}\mathrm{C}\,(\mathrm{p}\,,\gamma)\,^{13}\mathrm{N}$ and $^{13}\mathrm{C}\,(\mathrm{p}\,,\gamma)\,^{14}\mathrm{N}$ contribute for more than 70% of the total nuclear energy at the center of the star. We can thus write that $\epsilon_0 \propto Z \times X$, which leads to, using Eqs. A6 and A7,

$$\Delta\log\epsilon_0 = \left(\frac{1}{Z} - \frac{3.4}{X}\right)\frac{1}{\ln 10}\Delta Z \quad \text{(A10)}$$

Eqs. A3 and A4 become with Eqs. A5, A8, A9 and A10, and taking $X = 0.70$, $\mu = 0.617$ for $Z = 0.02$ and $X = 0.42$, $\mu = 0.80$ for $Z = 0.1$,

$$\frac{\Delta\log L}{\Delta\log Z} = \begin{cases}0.41-0.50-0.07 = -0.16 & Z = 0.02\\ 2.81-0.62-0.02 = \ 2.17 & Z = 0.10\end{cases} \quad \text{(A11)}$$

$$\frac{\Delta\log T_{eff}}{\Delta\log Z} = \begin{cases}0.09-0.16-0.09 = -0.16 & Z = 0.02\\ 0.79-0.20-0.02 = \ 0.57 & Z = 0.10\end{cases} \quad \text{(A12)}$$

We note from Eq. A11 the small effect of the nuclear production rate on the surface luminosity.

These relations should not be considered very accurate given the simplifications made in their derivation (mainly because of the departure of the opacity profile from the Kramers law and the resulting uncertainty in Eqs. A8 and A9). They however enable to understand qualitatively the ZAMS location of a $3\,\mathrm{M}_\odot$ star in the HR diagram as a function of the metallicity, and support the following conclusions found in Fig. 1:

- The surface luminosity at ZAMS is a decreasing function of Z at $Z = 0.02$ (and lower metallicities) and an increasing function of Z at $Z = 0.1$. The metallicity at which the inversion operates can only be determined from complete stellar model calculations and is found to be $Z \simeq 0.05$.

- The absolute shift $|\Delta\log L|$ resulting from an increase $\Delta\log Z$ is much greater at $Z = 0.1$ than at 0.02 (by a factor of about 14 according to Eq. A11). This result is qualitatively well verified by the ZAMS model calculations displayed in Fig. 1.

- The effective temperature is a decreasing function of Z for $Z \lesssim 0.05$, but it *increases* with metallicity for $Z \gtrsim 0.05$.

References

Alexander, D. R., Ferguson, J. W., 1994, ApJ 437, 879
Audouze J., 1987, Observational Cosmology, IAU Symp. 124, Eds. A. Hewitt et al., Reidel, p. 89
Charbonnel, C., Meynet, G., Maeder, A., Schaller, G., Schaerer, D., 1993, A&A Sup 101, 415 (Paper III)
Cox, J.P, Giuli, R.T., 1969, "Principles of Stellar Structure", Gordon and Breach, Science Publishers
Dorman, B., Rood, R.T., O'Connell, R.W., 1993, ApJ 419, 596
Fagotto, F., Bressan, A., Bertelli, G., Chiosi, C., 1994, A&A Sup 105, 39
Iglesias, C. A., Rogers, F. J., 1996, ApJ 464, 943
Iglesias, C. A., Rogers, F. J., Wilson, B. G., 1992, ApJ 397, 717
de Jager, C., Nieuwenhuijzen, H., van der Hucht K. A., 1988, A&AS 72, 259
Korista, K., Hamann, F., Ferguson, J., Ferland, G., 1996, ApJ 461, 641
Kudritzki, R.P., Pauldrach, A., Puls, J., Abbott, D. C., 1989, A&A 219, 205
Kurucz, R.L., 1991, in Stellar Atmospheres: Beyond Classical Models, NATO ASI Series C, Vol. 341
Langer N., 1989, A&A 220, 135
Langer N., Maeder, A., 1995, ApJ 450, L320
Maeder A., 1992, A&A 264, 105
Maeder A., 1998, in 'Abundance profiles: Diagnostic Tools for Galaxy History', eds. D. Friedli, M.G. Edmunds, C. Robert, L. Drissen, ASP Conf. Ser., in press
Maeder A., 1998, in 'Abundance Profiles: Diagnostic Tool for Galactic History', Eds. D. Friedly, M.G. Edmunds, C. Robert, L. Drissen, ASP Conf. Ser., in press
Maeder A., Conti P., 1994, ARA&A 32, 227
Maeder A., Lequeux J., 1982, A&A 114, 409
Maeder A., Meynet G., 1994, A&A 287, 803
Meynet, G., Maeder, A., Schaller, G., Schaerer, D., Charbonnel, C.: 1994, A&A Sup 103, 97 (Paper V)
Meynet, G., Mowlavi, N., Schaerer, D., Pindao, M.: 1998, IAU Symp. 184, in press
Mowlavi, N., 1995, Ph.D. Thesis (unpublished)
Mowlavi, N., Schaerer, D., Meynet, G., Bernasconi, P. A., Charbonnel, C., Maeder, A., in press (Paper VII)
Peimbert M., 1995, in The Light Element Abundances, Ed. P. Crane, Springer-Verlag, p. 165
Reimers, D., 1975, Mem. Soc. Sci. Liège 6th ser. 8, 369
Rogers, F. J., Iglesias, C. A., 1992, ApJ Sup. 79, 507
Schaerer, D., Charbonnel, C., Meynet, G., Maeder, A., Schaller, G., 1993, A&A Sup 102, 339 (Paper IV)
Schaerer, D., Meynet, G., Maeder, A., Schaller, G., 1993, A&A Sup 98, 523 (Paper II)
Schaller, G., Schaerer, D., Meynet, G., Maeder, A., 1992, A&A Sup 96, 269 (Paper I)
Simpson, J. P., Colgan, S. W., Rubin, R. H., Erickson, E. F., Haas, M. R., 1995, ApJ 444, 721
McWilliam, A., Rich, R. M., 1994, ApJS 91, 749